

---

# Moisture Migration through Exterior Envelopes in Brazil

**Nathan Mendes, Dr. Eng.**

**Roberto Lamberts, Ph.D.**

Associate Member ASHRAE

**Paulo Cesar Philippi, Dr. Ing.**

## ABSTRACT

An investigation of moisture migration through building envelopes has been made using the simulation software UMIDUS of transfer of heat and mass within porous walls in 13 Brazilian cities. Both diffusion and capillary regimes are taken into account; that is, the transfer of heat and mass through the material can be analyzed simultaneously for multi-layer walls. Both conditioned and unconditioned rooms are studied. The contribution of moisture migration to the ratio of latent heat flux to the total flux through the wall is calculated, and the importances of the role that moisture plays within the building envelope is analyzed. The effect of paint on the internal surface of the wall is investigated, and rain effects on the heat transfer are also discussed. It was found that an impermeable paint on the internal surface reduces the total heat transfer through the wall as it restricts moisture movement from the wall into the room.

---

## INTRODUCTION

Moisture flow through building envelopes affects the calculation of energy consumption in buildings, but normally, building simulation softwares assume that heat is transferred by pure conduction. However, most building materials are porous and therefore contain air and water in different phases. Walls are therefore subject to thermal and moisture gradients and the transfer of heat and mass occurs simultaneously and is interdependent. The transfer of moisture through common porous building materials, such as brick and mortar, depends on the complex morpho-topological characteristics of the pores in these materials.

Besides its effect on heat transfer, moisture has other implications, especially in hot/humid climates. It is well known that moisture can cause damage to the building structure and can promote the growth of mold and mildew, affecting the health of building occupants.

Several investigators have developed models to study heat and moisture transfer through porous building walls. Cunningham (1988) developed a mathematical model for hygroscopic materials in flat structures that uses an electrical

analogy with resistances for the vapor flow and an exponential approximation function with constant mass transport coefficients. Kerestecioglu and Gu (1989) investigated the phenomenon using evaporation-condensation theory in the pendular state (unsaturated liquid flow stage). The application of this theory is limited to low moisture content. Burch and Thomas (1991) developed a computational model, MOIST, using the finite-difference method to estimate the heat and mass transfer through composite walls under nonisothermal conditions. Thermal conductivity is normally considered constant, and the latent heat due to phase change within the wall was neglected. This program is also limited to low moisture content. El Diasty et al. (1993) used an analytical approach that assumed isothermal conditions and constant transport coefficients. Liesen (1994) used evaporation-condensation theory and a response factor method to develop and implement a model of heat and mass transfer in the building thermal simulation program IBLAST (Integrated Building Loads Analysis and System Thermodynamics). To use this method, hygrothermal property variations were neglected. There is no liquid transfer. This program is restricted to very low moisture content but has the

---

**Nathan Mendes** is an associate professor in the Department of Mechanical Engineering, Pontifical Catholic University of Paraná, Curitiba-PR, Brazil. **Roberto Lamberts** and **P.C. Philippi** are professors in the Civil Engineering Department and Mechanical Engineering Department, Federal University of Santa Catarina, Florianópolis-SC, Brazil.

advantage of short calculation time. Yik et al. (1995) developed a simplified model integrated with air-conditioning system component models that employs evaporation-condensation theory with differential permeability. It is a fast model but only applicable to materials that stay in the pendular state.

Thus, to study the dynamic effect of moisture on conductive heat transfer, it was decided to use the software *UMIDUS*. This software has been developed to model coupled heat and moisture transfer within porous building elements, avoiding limitations such as low moisture content, high computer run time, and low accuracy. Both diffusion and capillary regimes are taken into account; that is, the transfer of water in the vapor and liquid phases through the material can be analyzed for any kind of climate. The model predicts moisture and temperature profiles within multi-layer walls for any time step and calculates heat and mass transfer. Input files containing hourly data provide information on the conditions at the interior and exterior of the wall. A library of material properties is also available. The orientation and tilt of the wall are considered, and convection coefficients at the exterior of the wall are calculated hourly from wind velocity and direction data. The software allows the simulation of walls that have paint surfaces. The development and philosophy of *UMIDUS* are discussed by Mendes et al. (1999).

The aim of this study was to investigate the interdependence between moisture migration and weather conditions and their effects on conductive heat transfer within brick and mortar walls—which are widely used in Brazil—when subjected to the climatic conditions of 13 Brazilian cities and to identify a strategy to reduce the cooling load through hygroscopic walls in air-conditioned buildings by the use of an impermeable coat of paint on the internal surface of the wall. Both conditioned and unconditioned rooms were considered.

## MATHEMATICAL FORMULATION

The governing partial differential equations used in *UMIDUS* are given by Equations 1 and 2. They were derived from conservation of mass and energy flow in an elemental volume of porous material.

### Energy Conservation Equation.

$$\rho_0 c_m(T, \theta) \frac{\partial T}{\partial t} = \frac{\partial}{\partial x} \left( \lambda(T, \theta) \frac{\partial T}{\partial x} \right) - L(T) \frac{\partial}{\partial x} (j_v) \quad (1)$$

### Mass Conservation Equation.

$$\frac{\partial \theta}{\partial t} = \frac{\partial}{\partial x} \left( \frac{j}{\rho_l} \right) \quad (2)$$

Note that Equation 1 differs from Fourier's equation for transient heat flow by an added convective transport term (due to moisture diffusion associated with evaporation and condensation of water in the pores of the medium) and by a dependence on the moisture content (so that it is coupled to Equation 2). The driving forces for heat, liquid, and vapor transfer are temperature and moisture gradients. It was considered that the

one-dimensional assumption is adequate since both temperature and moisture gradients are much higher in the  $x$  direction. However, this assumption should not be considered in cases such as transfer through soils and in geometry configurations where corners play a significant role due their proximity.

The vapor flow and total flow (vapor plus liquid) are expressed in terms of transport coefficients  $D$  associated with the thermal and moisture gradients. According to Philip and DeVries (1957), the equations are:

For vapor flow,

$$\frac{j_v}{\rho_l} = -D_{Tv}(T, \theta) \frac{\partial T}{\partial x} - D_{\theta v}(T, \theta) \frac{\partial \theta}{\partial x}. \quad (3)$$

For total (vapor plus liquid) flow,

$$\frac{j}{\rho_l} = D_T(T, \theta) \frac{\partial T}{\partial x} - D_\theta(T, \theta) \frac{\partial \theta}{\partial x}. \quad (4)$$

Observe that the model does not take into account the gravity influence on the transfer of liquid water. This effect is very small compared to the capillary effect, especially for microporous materials. Note also that contributions of natural and forced convection heat transfer were not taken into account, which delimits the use of the model for high porosity insulation materials such as media filled with polystyrene pellets, cellulose, and mineral wool.

## Boundary Conditions

The associated conservation equations at the outside and inside wall surface are as follows. For the outside surface ( $x = 0$ ), it was considered that the wall is exposed to short-wave radiation, convective heat and mass transfer, and phase change. Thus, the energy balance becomes

$$\begin{aligned} & - \left( \lambda(T, \theta) \frac{\partial T}{\partial x} \right)_{x=0} - (L(T) j_v)_{x=0} \\ & = h(T_\infty - T_{x=0}) + \alpha q_r + L(T) h_m (\rho_{v,\infty} - \rho_{v,x=0}) \end{aligned} \quad (5)$$

where  $h(T_\infty - T_{x=0})$  represents the heat exchanged with the outside air, described by the convective heat transfer coefficient  $h$ ,  $\alpha q_r$  is the absorbed short-wave radiation, and  $L(T) h_m (\rho_{v,\infty} - \rho_{v,x=0})$ , the phase change energy term. The solar absorptivity is defined as  $\alpha$  and the mass convection coefficient as  $h_m$ , which is related to  $h$  by Lewis' relation.

The mass balance at the outside surface ( $x = 0$ ) is described as

$$-\frac{\partial}{\partial x} \left( D_\theta(T, \theta) \frac{\partial \theta}{\partial x} + D_T(T, \theta) \frac{\partial T}{\partial x} \right)_{x=0} = \frac{h_m}{\rho_l} (\rho_{v,\infty} - \rho_{v,x=0}). \quad (6)$$

The same equations apply to the inside surface ( $x = L$ ), with no short-wave terms.

The accuracy of the model depends considerably on the material properties. For hygroscopic walls, for example, simplifications of the model can result in large errors.

**TABLE 1**  
**Dimensions of the Standard Brick and Mortar Wall**

| Layer          | Thickness and Material  |
|----------------|-------------------------|
| External layer | 0.39 in. (10 mm) mortar |
| Mid layer      | 3.94 in. (100 mm) brick |
| Internal layer | 0.39 in. (10 mm) mortar |

**TABLE 2**  
**Dry Material Properties**

| Property                        | Brick  | Mortar |
|---------------------------------|--------|--------|
| $\rho_0$ [lbm/ft <sup>3</sup> ] | 118.61 | 127.98 |
| $\lambda$ (Btu/h·ft·°F)         | 0.64   | 1.13   |
| $C_m$ [Btu/lbm·°F]              | 0.22   | 0.23   |
| Open porosity                   | 0.29   | 0.18   |

## MATERIAL PROPERTIES

In most parts of Brazil, the walls are usually composed of three layers: lime mortar, brick, and lime mortar. Table 1 shows the dimensions of the vertical wall element that was modeled.

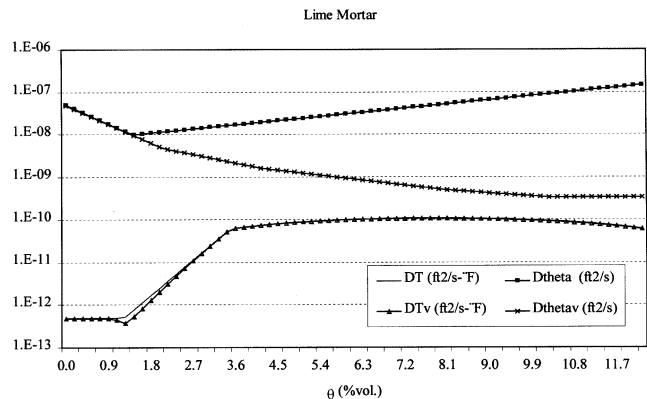
The basic dry material properties are given in Table 2. In this table “open porosity” is the ratio of the volume of open pores (i.e., pores with openings that have a path to both wall surfaces) to the total volume.

The available material data gathered from Perrin (1985) allows all the transport coefficients to be modeled as a function of moisture content. Figures 1 through 6 show the property data for both materials; however, they are slightly different from those presented by Perrin (1985) because fitting coefficients were applied on his experimental data. Instead of calculating all coefficients at each iteration, the program *UMIDUS* reads them from files, which speeds up simulations considerably.

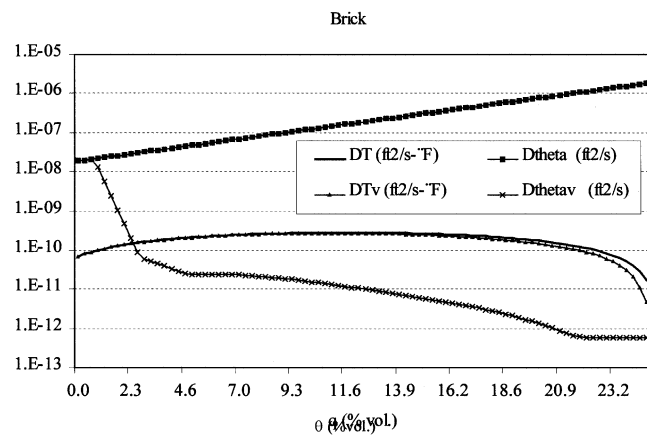
In Figures 1 and 2, vapor and total (liquid plus vapor) transport coefficients for lime mortar and brick are shown respectively. It is possible to see from Figures 1 and 2 that the coefficient responsible for the flow of liquid due to a temperature gradient ( $D_{TL}$ ) is very small compared to the one for vapor since the differences between the curves of  $D_T$  and  $D_{Tv}$  are very small.

Figure 3 presents the thermal conductivity curves for both materials. In those curves the vapor diffusion and phase change effects were not considered, which means they show the value for pure thermal conductivity for heat transfer conduction in the Fourier’s law.

Figure 4 presents the sorption isotherms curves for both materials. These curves are the average between adsorption and desorption curves. It is possible to notice from Figure 4 that lime mortar is more hygroscopic than brick.



**Figure 1** Mass transport coefficients for lime mortar.



**Figure 2** Mass transport coefficients for brick.

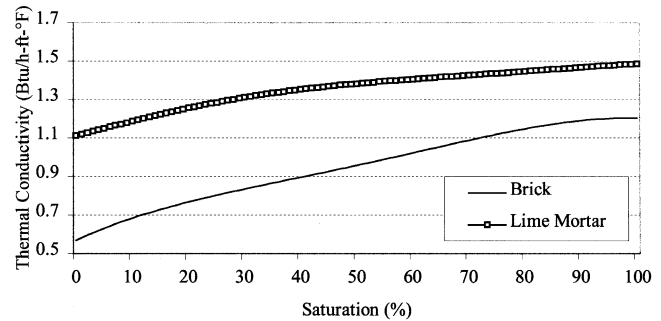


**Figure 3** Thermal conductivity for brick and lime mortar.

## SIMULATIONS

The *UMIDUS* model is solved with a finite-volume approach that uses a fully implicit solution scheme with coupling between the conservation equations. Using the Patankar (1980) method with uniform nodal spacing and a generic tridiagonal-matrix solution algorithm (Mendes 1997), the code solves the temperature and moisture content distributions simultaneously at each time step. Figure 5 shows the *UMIDUS* program interface.

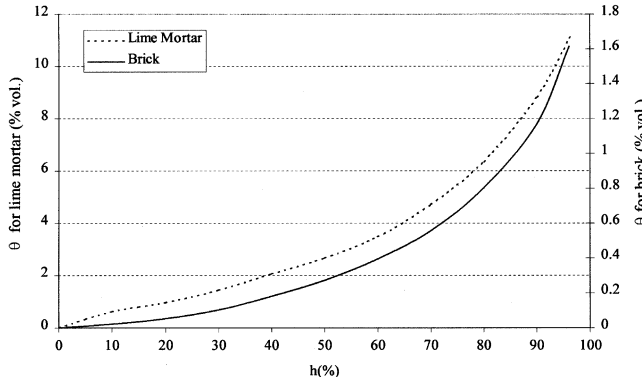


**Figure 4** Sorption isotherm curves for brick and lime mortar.

The vertical wall is south facing, as it represents a critical situation for moisture transfer, specially for the cities in the south (Porto Alegre, Florianopolis, and Curitiba). The external coefficient of convection was fixed at 2.18 Btu/h·ft<sup>2</sup>°F (12.4 W/m<sup>2</sup>k) and the internal 0.63 Btu/h·ft<sup>2</sup>°F (3.6 W/m<sup>2</sup>k). The reflectance of the ground in front of the wall was 0, and the solar absorbtivity of the external surface of the wall was 0.35. The permeance of a latex paint on the external and internal faces is 3.3 and 15.8 grain/h·ft<sup>2</sup>·in. Hg (190 and 900 ng/m<sup>2</sup>·s·Pa), respectively (Burch and Thomas 1991).

UMIDUS uses an external weather file to provide data input of the conditions at the exterior surface of the wall. The weather file contains the following variables: dry-bulb temperature, relative humidity, direct normal radiation, diffuse radiation, solar altitude, solar azimuth, wind speed, and wind direction. Each file contains 8760 hourly data points.

Weather files were produced from Test References Year (TRY) weather files for the following 13 Brazilian cities: Belém, Belo Horizonte, Brasília, Curitiba, Florianópolis, Fortaleza, Maceio, Natal, Porto Alegre, Recife, Rio de Janeiro, Salvador, and Vitória.

The internal condition file consists of two data items: dry-bulb temperature and relative humidity. Two sets of internal condition files were independently obtained as:

1. *Non-Conditioned* for a free running room using the building simulation program TRNSYS.
2. *Conditioned* for a room with an air-conditioning unit that functioned during office hours (24°C and 50%), using the simulation program VisualDOE.

It was considered for the building that each of its room has an area of 1162.1 ft<sup>2</sup> (108 m<sup>2</sup>) and a volume of 11428.8 ft<sup>3</sup> (324 m<sup>3</sup>). The external wall has a total area of 387.4 ft<sup>2</sup> (36 m<sup>2</sup>) of which 129.12 ft<sup>2</sup> (12 m<sup>2</sup>) is glazed. The air infiltration rate is 0.6.ach<sup>-1</sup> and the room was considered with no internal gains.

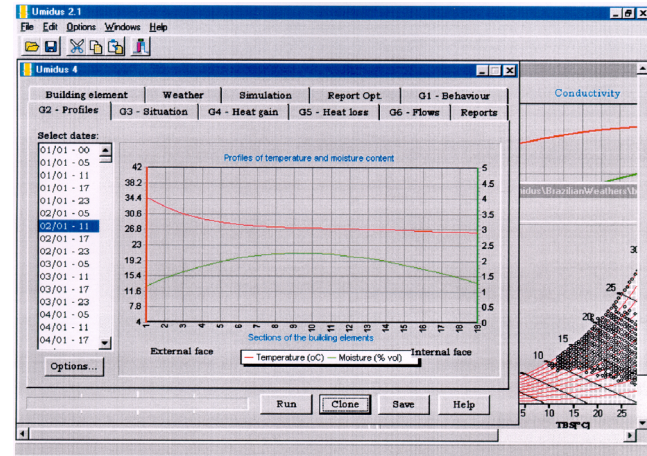


**Figure 5** The UMIDUS program showing temperature and moisture content profiles within a 10 cm brick wall on January 2 in the city of Curitiba.

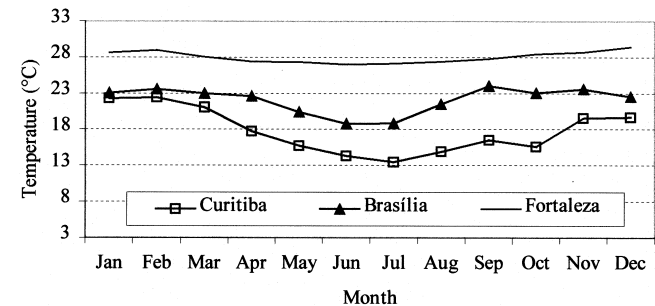


**Figure 6** Average wall temperature for the cities of Curitiba, Brasilia, and Fortaleza.

## RESULTS AND DISCUSSIONS

Simulations were performed for the 13 cities for both the conditioned and unconditioned cases. Spatial distribution of moisture content and temperature and heat fluxes was calculated. Simulations of the conditioned case were then repeated, but the paint on the internal surface of the wall was removed.

First, the moisture content profiles for brick and mortar walls in Curitiba (cold and humid), Brasília (hot and dry), and Fortaleza (hot and humid) are shown in Figures 6 through 10. The simulations are for the unconditioned case without inside paint. The reader can find the input files for internal conditions (temperature and relative humidity) in the UMIDUS folder. Figures 6 and 7 show the temperature and moisture content average over the thickness of the wall during the whole year.

Note in Figure 6 that the average temperature within the wall in the city of Curitiba (-25.4°S) is considerably lower than those for Brasilia (-15.5°S) and Fortaleza (-3.5°S). As Fortaleza is very close to the equator line, the yearly thermal

amplitude is quite low, which reflects a stable and predominantly hot weather.

On the other hand, it is in Curitiba where the wall reaches the highest levels of moisture content as shown in Figure 7. This can be explained by the low vapor losses due to an unelated solar radiation. In Brasilia, the wall is dried out during the dry season (May–October).

Figures 8 through 10 present the moisture content profiles in the winter (June 15) and summer (December 15) for these three cities. Figure 8 illustrates the moisture content profile on a winter day (6/15) and on a summer day (12/15). In summer, as the weather does not change much from 6 a.m. to 6 p.m. in Brasília, there is not much difference between the moisture distribution from the early morning to the late afternoon. However, in winter (dry season), the temperature during the day goes up with a considerable amount of solar radiation, which causes the wall to loose water during the day and to take it in during the night.

Nevertheless, in Curitiba (Figure 9) the moisture content gradients are higher, which makes the moisture migration more relevant than in other Brazilian cities.

As it was perceived for Curitiba, the moisture content gradients are also high in Fortaleza (Figure 10). However, only

in Brasilia were higher moisture contents registered in summer because a strong dry season occurs between May and October.

Figure 11 illustrates a comparison of moisture content at the center of the wall for the three simulated cases for the city of Fortaleza. We notice from Figure 11 that the moisture content in the conditioned wall is approximately 50% that of the unconditioned wall. The conditioned room has a substantially lower relative humidity and lower summer temperatures. The air conditioner is effectively drying out the wall. We can also observe from the same figure that the moisture content is higher in the winter as expected.

Table 3 shows the results of the first simulation for an unconditioned building in Fortaleza with paint on the internal surface in terms of monthly integrated heat fluxes, wall moisture content, and temperature at the center of the wall. The subscript  $p$  means that heat goes from outside to inside and vice versa for the subscript  $n$ .

We see from Table 3 that heat goes from outside to inside most of time, as Fortaleza is a predominantly hot weather city, and that the moisture content within the wall is higher during the winter since the vapor concentration difference between the wall surfaces and air is lower due to a lower air temperature.

Table 3 also shows the results of the second simulation for a conditioned building in Fortaleza with paint on the internal surface in terms of monthly integrated heat fluxes, moisture content, and temperature at the center of the wall. We notice from Table 3 that the positive sensible heat for a conditioned building is considerably higher than that showed for an unconditioned one, especially in summer (October – March) where the temperature difference between inside and outside is much higher for a conditioned building. As the air conditioning dries out the wall, the moisture content decreases and the monthly averaged latent heat tends to reduce. Mendes et al. (1996) showed that large errors in sensible and latent heat transfer can result if moisture migration and the dependence of thermal properties on moisture content are neglected. The errors are largest in the morning when the cooling system turns on and

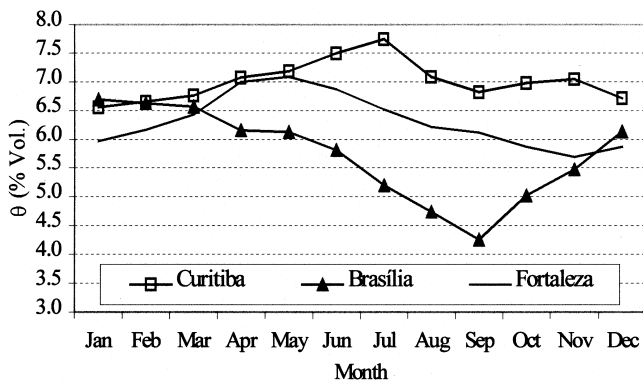


Figure 7 Average moisture content for the cities of Curitiba, Brasilia, and Fortaleza.

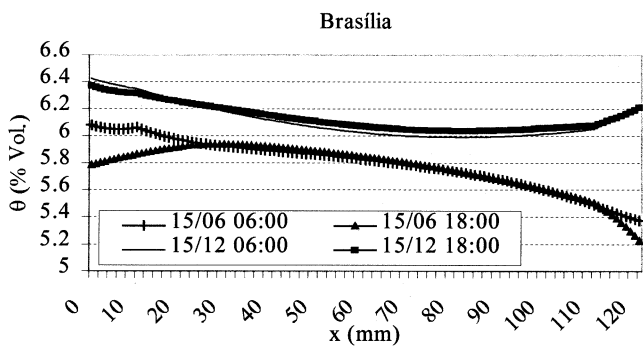


Figure 8 Moisture content profile for the city of Brasília.

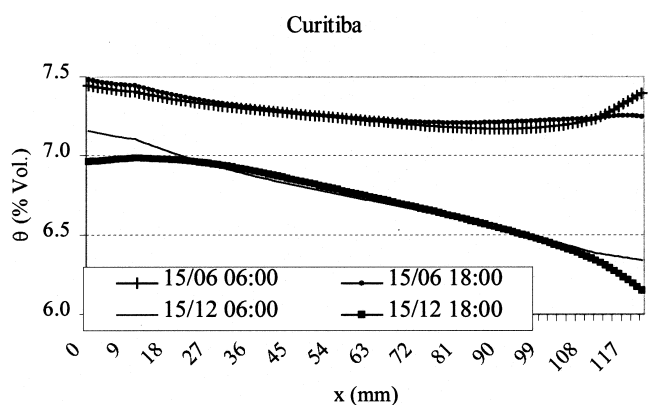


Figure 9 Moisture content profile for the city of Curitiba.

**TABLE 3**  
**Monthly Integrated Heat Fluxes and Temperature at Center of Wall for an Unconditioned Building, for a Conditioned Building, and for a Conditioned Building with No Paint in the City of Fortaleza**

| Month | Unconditioned |             |       | Conditioned |             |       | Conditioned with no paint |             |       |
|-------|---------------|-------------|-------|-------------|-------------|-------|---------------------------|-------------|-------|
|       | $Q_{s,p}^*$   | $Q_{l,p}^*$ | T**   | $Q_{s,p}^*$ | $Q_{l,p}^*$ | T**   | $Q_{s,p}^*$               | $Q_{l,p}^*$ | T**   |
| Jan   | 0.657         | 0.063       | 91.27 | 1.655       | 0.027       | 90.52 | 1.658                     | 0.221       | 90.52 |
| Feb   | 0.559         | 0.042       | 91.18 | 1.522       | 0.021       | 90.18 | 1.526                     | 0.150       | 90.18 |
| Mar   | 0.629         | 0.030       | 88.66 | 1.495       | 0.017       | 88.16 | 1.502                     | 0.139       | 88.16 |
| Apr   | 0.428         | 0.017       | 85.91 | 1.054       | 0.013       | 85.93 | 1.061                     | 0.138       | 85.93 |
| May   | 0.274         | 0.014       | 83.55 | 0.764       | 0.010       | 83.55 | 0.774                     | 0.122       | 83.57 |
| Jun   | 0.079         | 0.016       | 80.46 | 0.323       | 0.005       | 80.64 | 0.329                     | 0.083       | 80.64 |
| Jul   | 0.089         | 0.017       | 80.40 | 0.351       | 0.009       | 80.64 | 0.356                     | 0.122       | 80.62 |
| Aug   | 0.075         | 0.040       | 81.10 | 0.341       | 0.010       | 80.98 | 0.345                     | 0.114       | 80.98 |
| Sep   | 0.116         | 0.046       | 84.29 | 0.715       | 0.020       | 83.93 | 0.723                     | 0.138       | 83.91 |
| Oct   | 0.335         | 0.094       | 88.29 | 1.250       | 0.035       | 87.64 | 1.253                     | 0.229       | 87.62 |
| Nov   | 0.637         | 0.094       | 90.90 | 1.728       | 0.041       | 89.67 | 1.728                     | 0.303       | 89.65 |
| Dec   | 0.582         | 0.068       | 92.48 | 1.804       | 0.034       | 90.93 | 1.805                     | 0.243       | 90.91 |

**TABLE 4**  
**Contribution of Latent Heat to Total Heat  
for the 13 Cities in the Simulations**

| City           | % of latent heat to total |
|----------------|---------------------------|
| Belém          | 2.0                       |
| Belo Horizonte | 2.5                       |
| Brasília       | 4.3                       |
| Curitiba       | 18.2                      |
| Florianópolis  | 7.3                       |
| Fortaleza      | 1.8                       |
| Maceió         | 2.8                       |
| Natal          | 2.2                       |
| Porto Alegre   | 8.5                       |
| Recife         | 2.1                       |
| Rio de Janeiro | 3.9                       |
| Salvador       | 1.5                       |
| Vitória        | 4.3                       |

a large latent load due to moisture extracted from the walls can occur.

We see from Table 4 that in colder and more humid cities, especially in the southern part of the country (Curitiba, Porto Alegre, and Florianópolis), the contribution of latent heat on the total is more significant. In the cities in the northeast region, there is a very high heat flux into the building once they are predominantly hot.

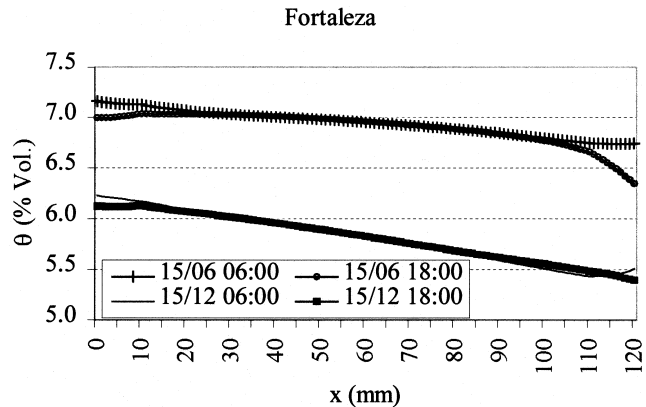


**Figure 10** Moisture content profile for the city of Fortaleza.

In Table 4, the contribution of latent heat to total heat for the 13 cities is presented, and we can note the importance of the moisture migration, especially for the cities in the south (Curitiba, Florianópolis, and Porto Alegre) where the moisture contents are higher.

## CONCLUSIONS

This study has shown that the fact of having no paint on the internal wall surface increases the latent loads significantly, and the sensible heat flux is slightly higher than for the painted internal surface. The most important result is the heat flow through the wall in the positive direction; that is, the cooling load is smaller for the case when the internal surface of the

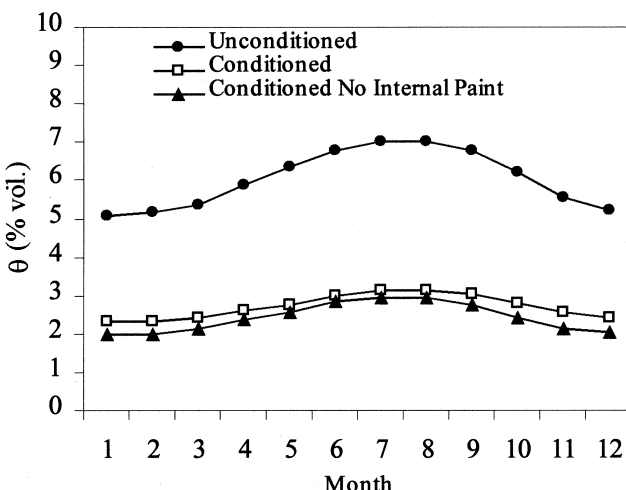


**Figure 11** Monthly average moisture content at the center of the wall for the three simulated cases.

wall is painted. The impermeable paint inhibits the movement of moisture between the room and the wall.

The comparison between a painted wall and an unpainted wall is perhaps not so useful, as in most situations the internal surfaces of the room will be painted. The more useful observation is that reducing the permeability of the internal surface reduces the cooling load. If the permeability of the paint is further reduced to 0, by the application of a thick latex or silicon sealing agent, the flux of latent heat into the room could be eliminated, thus reducing the total cooling load. In the case of Fortaleza, a complete impermeable barrier on the internal surface could reduce the annual conductive cooling load by a further 1.8%.

We observed from the contribution of latent heat to total heat, for the 13 Brazilian cities, the importance of the moisture migration, especially for the cities in the south (Curitiba, Florianópolis, and Porto Alegre) where the moisture contents are higher.

In conclusion, we have shown the important interaction of moisture migration, climate, hygroscopic building materials, and paint on the determination of conductive heat transfer through a porous wall and that UMIDUS is a useful tool for modeling the coupled transfer of heat and mass through hygroscopic materials with painted surfaces.

## ACKNOWLEDGMENTS

The authors thank CNPq - Conselho Nacional de Desenvolvimento Científico e Tecnológico (Brazilian Research Council) of the Ministry for Science and Technology of Brazil for the support of this work.

## NOMENCLATURE

|           |  |
|-----------|--|
| $c$       | = specific heat  |
| $D_{T_v}$ | = vapor phase transport coefficient associated with a temperature gradient |

|                |   |
|----------------|---|
| $D_{\theta_v}$ | = vapor phase transport coefficient associated with a moisture content gradient |
| $D_T$          | = mass transport coefficient associated with a temperature gradient             |
| $D_\theta$     | = mass transport coefficient associated with a moisture content gradient        |
| $h$            | = convective heat transfer coefficient  |
| $h_m$          | = vapor transfer coefficient in air   |
| $j$            | = total (vapor plus liquid) flow  |
| $j_v$          | = vapor flow  |
| $L$            | = heat of vaporization, wall thickness  |
| $q_r$          | = short-wave solar radiation  |
| $Q_{s,p}$      | = monthly integrated sensible heat flux into building through wall              |
| $Q_{l,p}$      | = monthly integrated latent heat flux into building through wall                |
| $T$            | = temperature   |
| $t$            | = time  |
| $x$            | = distance into wall  |
| $\alpha$       | = solar thermal radiation absorptance   |
| $\lambda$      | = thermal conductivity  |
| $\theta$       | = total moisture volumetric content (vol. of water / vol. of porous material)   |
| $\rho$         | = mass density  |

## Subscripts

|     |                |
|-----|----------------|
| $l$ | = liquid       |
| $m$ | = mean         |
| $o$ | = solid matrix |
| $v$ | = vapor        |

## REFERENCES

- Burch, D.M., and W.C. Thomas. 1991. *An analysis of moisture accumulation in wood frame wall subjected to winter climate*, NISTIR 4674. Gaithersburg, Md.: National Institute of Standards and Technology.
- Cunningham, M.J. 1988. The moisture performance of framed structures: A mathematical model. *Bldg Environ.* 23: 123 - 135.
- El Diasty, R., P. Fazio, and I. Budaiwi. 1993. Dynamic modelling of moisture absorption and desorption in buildings. *Bldg Environ.* 28: 21-32.
- Kerestecioglu, A., and L. Gu. 1989. Incorporation of the effective penetration depth theory into TRNSYS, draft report. Cape Canaveral: Florida Solar Energy Center.
- Liesen, R.J. 1994. Development of a response factor approach for modeling the energy effects of combined heat and mass transfer with vapor adsorption in building elements. Ph.D. thesis, Mechanical Engineering Department, University of Illinois.
- Mendes, N., F.C. Winkelmann, R. Lamberts, P.C. Philipp, and J.A.B. Cunha Neto. 1996. Dynamic analysis of

- moisture transport through walls and associated cooling loads in the hot/humid climate of Florianópolis, Brazil. *10th Symposium on Improving Building Systems in Hot and Humid Climates*, pp. 253-261. Fort Worth, Texas: EUA.
- Mendes, N. 1997. *Models for predicting heat and moisture transfer in porous building elements*. Ph.D. thesis, Federal University of Santa Catarina, Florianópolis, Brazil (in Portuguese).
- Mendes, N., I. Ridley, R. Lamberts, P.C. Philippi, and K. Budag. 1999. UMIDUS: A PC program for the prediction of heat and moisture transfer in porous building elements. *Building Simulation Conference – IBPSA 99*, pp. 277-283. Kyoto.
- Patankar, S.V. 1981. *Numerical heat transfer and fluid flow*. New York: McGraw-Hill.
- Perrin, B. 1985. Etude des transferts couplés de chaleur et de masse dans des matériaux poreux consolidés non saturés utilisés en génie civil. Thèse Docteur d'Etat. Toulouse, Universite Paul Sabatier de Toulouse.
- Philip, J.R., and D.A. De Vries. 1957. Moisture movement in porous materials under temperature gradients. *Transactions of the American Geophysical Union* 38(2): 222-232.
- Yik, F.W.H., C.P. Underwood, and W.K. Chow. 1995. Simultaneous modelling of heat and moisture transfer and air-conditioning systems in buildings. *Proc. IBPSA Building Simulation '95, 4th International Conference*. Madison, Wis.